Available online at www.sciencedirect.com
ScienceDirect
Inorganica Chimica Acta 360 (2007) 1200–1208
Inorganica Chimica Acta
www.elsevier.com/locate/ica

Synthesis and photophysical properties of dansyl-based polyamine ligands and their Zn(II) complexes

A. Jorge Parola [a,*], João Carlos Lima [a], Fernando Pina [a], João Pina [b], João Seixas de Melo [b], Conxa Soriano [c], Enrique García-España [d,*], Ricardo Aucejo [d], Javier Alarcón [e]

[a] *REQUIMTE, Departamento de Química, Faculdade de Ciências e Tecnologia, Universidade Nova de Lisboa, 2829-516 Monte de Caparica, Portugal*
[b] *Departamento de Química, Faculdade de Ciências e Tecnologia, Universidade de Coimbra, 3004-535 Coimbra, Portugal*
[c] *Departament de Química Orgánica, ICMOL, Facultat Farmacia, Universitat de València, 46100 Burjassot (Valencia), Spain*
[d] *Departament de Química Inorgànica, ICMOL, Universitat de València, Apdo Correos 22085, 46071 Burjassot (Valencia), Spain*
[e] *Departament de Química Inorgànica, Universitat de València, Cl Dr. Moliner 50, 46100 Burjassot (Valencia), Spain*

Received 10 October 2006; accepted 5 November 2006
Available online 12 November 2006

Dedicated to Professor Vincenzo Balzani.

Abstract

The synthesis, potentiometric studies and photophysical properties of two new polyamine ligands (**L1** and **L2**) possessing the dansyl chromophore were studied in aqueous 0.15 M NaCl. The compounds show the absorption and emissions bands characteristic of the dansylamide fluorophore and both present intramolecular excited state proton transfer at intermediate pH ranges. One of the ligands (**L2**) strongly coordinates Zn(II) leading to fluorescence quenching. A model compound (**L3**) of the dansyl moiety was also investigated.
© 2006 Elsevier B.V. All rights reserved.

Keywords: Dansyl; Polyamine ligands; Pyridine ligands; Zn(II) complexes; Chemosensors; Fluorescence

1. Introduction

Fluorescent polyamine chemosensors for the detection of metal ions have received considerable interest due to their potential applications in a variety of fields, such as analytical chemistry and clinical biochemistry [1–3]. These ligands have also been largely explored for the detection of anions, using essentially two different approaches: binding by protonated polyamine ligands and, complexation to coordinatively unsaturated metal complexes of the ligands [4–6].

The dansyl fluorophore (5-dimethylamino-1-naphthalenesulfonate) is characterized by a charge transfer excited state exhibiting solvatochromism and high emission quantum yields [7]. These characteristics, together with the synthetic flexibility of the sulfonic acid group, have led the dansyl fluorophore to be a core-structure present in many fluorescent sensors and labels for the detection of both metal cations [8–10] and anions [11–13] as well as in larger supramolecular structures such as dendrimers [14].

In this work, we present the synthesis of dansyl labelled ligands **L1** and **L2**, as well as model compound **L3**. Ligand **L1** is an intermediate product in the synthesis of **L2** that poorly binds metal cations but should be able to bind some highly charged anions, like phosphates. Ligand **L2**, on the other hand, has four pre-organized nitrogen atoms to bind metal ions leaving free one or two coordination sites to be

* Corresponding authors. Tel.: +351 212948300; fax: +351 212948550 (A.J. Parola); tel.:/fax: +34 963544879 (E. García-España).
E-mail addresses: ajp@dq.fct.unl.pt (A.J. Parola), enrique.garcia-es@uv.es (E. García-España).

0020-1693/$ - see front matter © 2006 Elsevier B.V. All rights reserved.
doi:10.1016/j.ica.2006.11.006

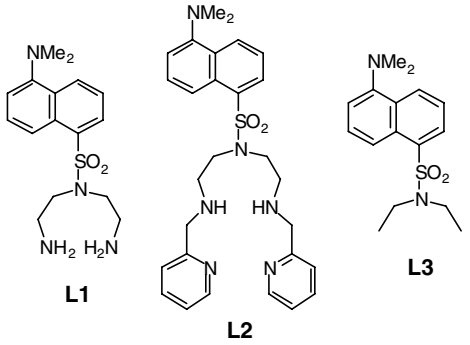

Scheme 1.

explored for anion detection. Prior to the study of anion binding by **L1** and **L2**, a photophysical characterization of both ligands, of the Zn(II) and Cu(II) complexes of **L2**, as well as of model compound **L3** are required, since photoinduced processes are expected to be affected by the presence of bound anions (Scheme 1).

2. Experimental

2.1. Synthesis

All reagents and solvents used were of analytical grade. NMR spectra were run on a Bruker AMX 400 instrument and elemental analyses were obtained on a Thermofinnigan Flash EA 1112 Series device.

Synthesis of 1,5-phthalimido-3-azapentane (**1**) (see Scheme 2) was carried out as described in Ref. [15].

2.1.1. 3-Dansyl-1,5-diphthalimido-3-azapentane (*2*) [16,17]

1,5-Phthalimido-3-azapentane (**1**) (2.7 g, 8 mmol), dansyl chloride (2.5 g, 9.3 mmol) and K_2CO_3 (1.3 g, 9.3 mmol) were dissolved in 200 mL of CH_3CN. The mixture was refluxed for 24 h under a nitrogen atmosphere. After filtration, the solvent was removed under reduced pressure. The resulting residue was mixed with 50 mL of water and extracted with dichloromethane (3×50 mL). The organic phase was dried with anhydrous sodium sulfate and the solvent was evaporated to yield a light yellow oil. The oil was taken in EtOH and precipitated as a solid (3-dansyl-1,5-diphthalimido-3-azapentane) **2** which was filtered. Yield: 1.96 g, 41%. ^{1}H NMR (D_2O): δ (ppm) 2.63 (s, 6H), 3.78–3.88 (m, 8H), 6.61 (d, 1H, $J = 7$ Hz), 7.12–7.18 (dd, 1H, $J = 9$ Hz), 7.28–7.33 (dd, 1H, $J = 9$ Hz), 7.55 (br s, 8H), 7.70 (d, 1H, $J = 9$ Hz), 8.03–8.06 (dd, 1H, $J = 7$ Hz), 8.85 (d, 1H, $J = 8$ Hz).

2.1.2. 4-Dansyl-1,4,7-triazaheptane (*L1 · 3HCl*)

3-Dansyl-1,5-diphthalimido-3-azapentane (**2**) (1.8 g, 4.3 mmol) and hydrazine monohydrate (2.8 g, 87 mmol) were dissolved in 200 mL of EtOH. The mixture was refluxed for 1 day under a nitrogen atmosphere. The precipitate was removed by filtration and the solvent was evaporated until the sample was dry. The resulting residue was dissolved in 200 mL of $CHCl_3$ and the solution was stirred for 12 h under a nitrogen atmosphere. The solution

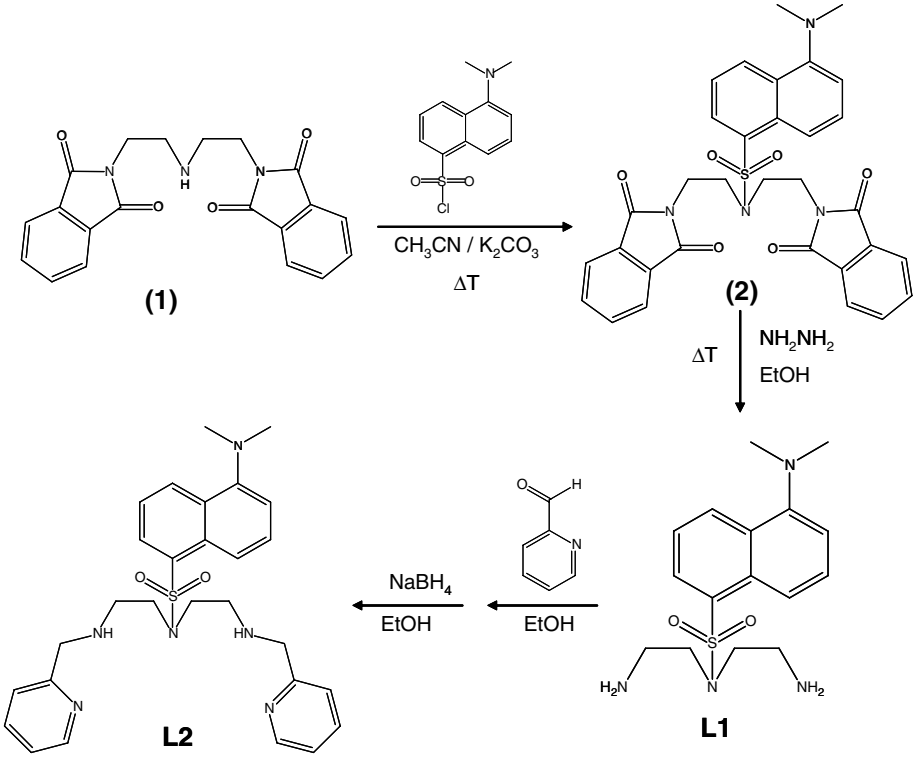

Scheme 2.

was vacuum evaporated to dryness to give the crude product. This product was dissolved in EtOH and was precipitated with aqueous HCl to obtain **L1** as its trihydrochloride salt (0.84 g, 44%). Mp 223–224 °C. ^{1}H NMR (D_2O): δ (ppm) 3.25 (t, 4H, $J = 6$ Hz), 3.46 (s, 6H), 3.74 (t, 4H, $J = 6$ Hz), 7.89 (t, 1H, $J = 8$ Hz), 8.06 (d, 1H, $J = 8$ Hz), 8.16 (d, 1H, $J = 8$ Hz), 8.45 (d, 1H, $J = 9$ Hz), 8.79 (d, 1H, $J = 9$ Hz). ^{13}C NMR (D_2O): δ (ppm) 39.04, 47.05, 48.27, 120.13, 126.64, 126.85, 127.32, 128.84, 129.33. *Anal.* Calc. for $C_{16}H_{29}N_4Cl_3SO_3$: C, 41.4; H, 6.3; N, 12.1. Found: C, 40.9; H, 6.2; N, 12.2%.

2.1.3. 4-Dansyl-1,7-(2-methylpyridine)-1,4,7-triazaheptane (*L2* · 5HCl)

2-Pyridine-carbaldehyde (0.61 g, 5.7 mmol) dissolved in 100 mL of EtOH was added to a solution of 4-dansyl-1,4,7-triazaheptane (**L1**) (0.96 g, 2.85 mmol) in EtOH. $NaBH_4$ (0.43 g, 11 mmol) was then added portion wise. The mixture was stirred for 2 h at room temperature and the solvent was vacuum evaporated to dryness. The residue was treated with 50 mL of water and extracted with CH_2Cl_2 (3×40 mL). The organic phase was dried with anhydrous sodium sulfate and the solvent evaporated to dryness. The resulting oil was dissolved in EtOH and **L2** was precipitated as its pentahydrochloride salt with aqueous HCl (1.55 g, 41 %). Mp 177–178 °C. ^{1}H NMR (D_2O): δ (ppm) 3.47 (t, 4H, $J = 6$ Hz), 3.51 (s, 6H), 3.92 (t, 4H, $J = 6$ Hz), 4.48 (s, 4H), 7.53–7.59 (m, 4H), 7.91–7.96 (m, 2H), 7.99 (t, 1H, $J = 9$ Hz), 8.00 (t, 1H, $J = 8$ Hz), 8.12 (d, 1H, $J = 8$ Hz), 8.24 (d, 1H, $J = 8$ Hz), 8.52 (d, 1H, $J = 9$ Hz), 8.61 (d, 1H, $J = 5$ Hz), 8.83 (d, 1H, $J = 9$ Hz). ^{13}C NMR (D_2O): δ (ppm) 46.7, 46.9, 47.1, 50.4, 125.4, 125.8, 126.7, 126.9, 127.4, 128.9, 129.1, 129.5, 141.4, 148.0, 148.7. *Anal.* Calc. for $C_{27}H_{40}N_5Cl_5O_2$: C, 50.5; H, 6.3; N, 10.9. Found: C, 50.6; H, 6.4; N, 10.8%.

2.1.4. 5-Dimethylaminonaphthalene-1-sulfonic acid diethylamide (*L3*)

Sodium hydroxide (100 mg, 2.5 mmol) was dissolved in 1 ml of water and diethylamine (62 μl, 0.6 mmol) was added. Dansyl chloride (135 mg, 0.5 mmol) was then added over a period of 5 min. After 2 h, no dansyl chloride was left. The mixture was diluted and extracted with 2×10 ml CH_2Cl_2. The organic phase was dried over Na_2SO_4, filtered, concentrated and purified by flash chromatography over silica gel, eluting with CH_2Cl_2. The product was isolated as a slightly yellow oil. ^{1}H NMR ($CDCl_3$) δ (ppm) 1.10 (t, 6H, $J = 7.1$ Hz, NCH_2CH_3), 2.91 (s, 3H, NCH_3), 3.37 (q, 4H, $J = 7.1$ Hz, NCH_2CH_3), 7.20 (d, 1H, $J = 7.1$ Hz), 7.53 (m, 2H), 8.18 (dd, 1H, $J = 7.3$ Hz, $J = 0.7$ Hz), 8.32 (d, 1H, $J = 8.5$ Hz), 8.57 (d, 1H, $J = 7.3$ Hz).

2.2. Emf measurements

The potentiometric titrations were carried out at 298.1 ± 0.1 K using NaCl 0.15 mol dm^{-3} as supporting electrolyte. The experimental procedure (burette, potentiometer, cell, stirrer, microcomputer, etc.) has been fully described elsewhere [18]. The acquisition of the emf data was performed with the computer program PASAT [19]. The reference electrode was an Ag/AgCl electrode in saturated KCl solution. The glass electrode was calibrated as a hydrogen-ion concentration probe by titration of previously standardized amounts of HCl with CO_2-free NaOH solutions and the equivalent point determined by the Gran's method [20], which gives the standard potential, $E^{\circ\prime}$, and the ionic product of water ($pK_w = 13.73(1)$).

The computer program HYPERQUAD was used to calculate the protonation and stability constants [21]. The pH range investigated was 2.0–11.0 and the concentration of the metal ions and of the ligands ranged from 1×10^{-3} to 5×10^{-3} mol dm^{-3} with M:L molar ratios 1:1. The different titration curves for each system (at least two) were treated either as a single set or as separated curves without significant variations in the values of the stability constants. Finally, the sets of data were merged together and treated simultaneously to give the final stability constants. The distribution diagrams were plotted with the HYSS program [22].

2.3. Spectroscopic and transient measurements

All experiments were carried out in 0.15 M NaCl aqueous solutions. The pH was adjusted by addition of HCl and NaOH, and was measured in a Meterlab pHM240 pH meter from Radiometer Copenhagen. The pK_a's associated with spectral changes were determined by global analysis of the pH dependent absorption spectra by using Specfit/32 Global Analysis System for Windows.

UV/Vis absorption spectra were recorded in a Shimadzu UV2501-PC spectrophotometer. Fluorescence spectra were recorded on a Jobin-Yvon Spex Fluorog 3-2.2 spectrofluorimeter an were corrected for the wavelength response of the system. Fluorescence quantum yields were determined using quinine sulfate in 1 M H_2SO_4 as standard ($\Phi = 0.546$) [23].

Fluorescence intensity decays were measured using a home built TCSPC apparatus [24] with 280 and 339 nm Horiba-JI-IBH nanoLED excitation, Jobin-Yvon monochromator, Philips XP2020Q photomultiplier, and Canberra instruments TAC and MCA and were analyzed using the method of modulating functions of Striker [25]. The time resolution of this equipment is 150 ps.

3. Results and discussion

3.1. Synthesis of ligands

Compound **L2** has been synthesised in a four step synthetic route which is depicted in Scheme 2. The first step is the protection of *N*1-(2-amino-ethyl)-ethane-1,2-diamine (*dien*) with phthalate groups to avoid the alkylation of the primary amino groups [15]. Introduction of the

fluorophore is then carried out by alkylation of the central nitrogen with dansyl chloride [16,17]. Removal of the phthalate groups is then achieved by treatment with hydrazine in ethanol that gives the free alkylated polyamine (**L1**), which is then precipitated as its hydrochloride salt. Condensation of **L1** with 2-pyridine-carbaldehyde in 1:2 mole ratio provides the precursor imine of **L2**, which is reduced *in situ* with $NaBH_4$. Finally, **L2** is precipitated as its hydrochloride salt by addition of aqueous HCl to an ethanolic solution of **L2**.

Model compound **L3** was synthesized to help in the interpretation of the photophysical properties of ligands **L1** and **L2**.

3.2. Potentiometric studies

Table 1 collects the stepwise basicity constants for polyamines **L1** and **L2** determined in 0.15 M NaCl by means of the computer program HYPERQUAD [21]. The first aspect that deserves to be mentioned is the low values of the protonation constants in comparison with related polyamines without the dansyl group. For instance, the analogous polyamine to **L1** containing naphthalene instead of dansyl as a fluorophore, displays much higher constants for the first two steps ($\log K_{HL/H\cdot L} = 9.79(1)$, $\log K_{H_2L/HL\cdot H} = 9.17(1)$), and a clearly lower constant for the third step ($\log K_{H_3L/H_2L\cdot H} = 2.37(2)$) [26]. This can be explained taking into account on the one hand the electron-withdrawing characteristics of the dansyl group which will reduce the basicity of the primary amines and on the other hand, that the third protonation in **L2** will be occurring at the dimethylamino function of the dansyl group. The value of 3.6 logarithmic units found for the protonation of dansyl agrees quite well with the values reported for similar ligands [27,28].

Compound **L2** presents a similar sequence of basicity constants than **L1**, with values of the first two protonation constants even lower. This further reduction in basicity can be attributed to the additional electron withdrawal produced by the pyridine rings. The constant for the protonation of the dimethylamino functionality has the same value than in the previous ligand which can be explained by the large separation existing between both protonation sites in the ligands. The protonation trend will be further discussed in the light of the photochemical studies (vide infra).

Table 1
Stepwise basicity constants for **L1** determined at 298.1 ± 0.1 K in 0.15 M NaCl

Reaction	log *K*	
	L1	**L2**
$L + H = LH$[a]	8.76 (1)[b]	7.98 (2)[b]
$LH + H = LH_2$	7.74 (1)	6.31 (2)
$LH_2 + H = LH_3$	3.62 (1)	3.76 (3)
$\log\beta$	20.12 (1)	18.05 (3)

[a] Charges ommited for clarity.
[b] Values in parentheses are standard deviations in the last significant figure.

Table 2
Stability constants for the formation of Zn(II) complexes of **L1** and **L2** determined in 0.15 M NaCl at 298.1 K

Reaction	log *K*	
	L1	**L2**
$L + 2H + Zn = ZnH_2L$[a]		17.49 (6)[b]
$L + H + Zn = ZnHL$		12.99 (6)
$L + Zn = ZnL$		8.38 (4)
$L + Zn + H_2O = ZnL(OH) + H$	−4.36 (1)[b]	−1.17 (5)
$L + Zn + 2H_2O = ZnL(OH)_2 + 2H$	−13.94 (2)	−11.54 (4)
$ZnHL + H = ZnH_2L$		4.50 (6)
$ZnL + H = ZnHL$		4.61 (2)

[a] Charges ommited for clarity.
[b] Values in parentheses are standard deviations in the last significant figure.

Table 2 gathers the stability constants for the Zn(II) complexes formed by **L1** and **L2** under our experimental conditions ($I = 0.15$ M NaCl, $T = 298.1$ K).

The stability data shows that **L1** binds poorly the Zn(II) ions; the only species found in aqueous solution are hydroxylated. The dansyl group blocks the coordinating ability of the central nitrogen and thus the binding to the metal ion results to be relatively weak. In the case of **L2**, the pyridine units will strength its capacity to bind the metal ion. Although the polyamine moiety might seem to be divided into two compartments which will be sharing the functionalized nitrogens, only mononuclear complexes have been detected.

3.3. Photophysical properties

Ligands **L1** and **L2** are characterized by the presence of the dansyl fluorophore which requires the study of model compound **L3**. All studies were made in 0.15 M NaCl aqueous solutions.

3.3.1. Model compound *L3*

The absorption spectra of compound **L3** as a function of pH are represented in Fig. 1. Analysis of the data (see inset in Fig. 1) allows to determine a $pK_a = 3.5$ that corresponds to the protonation of the dimethylamino group. This value compares well with the pK_a of the dimethylamino group in similar dansyl sulfonamide derivatives [27,28]. The absorption characteristics of the two different forms of compound **L3** are clearly perceived from Fig. 1: the protonated species has $\lambda_{max} = 285$ nm ($\varepsilon = 4700\ M^{-1}\,cm^{-1}$), resembling the characteristic absorption of naphthalene derivatives [29], while the unprotonated form is characterized by $\lambda_{max} = 325$ nm ($\varepsilon = 2400\ M^{-1}\,cm^{-1}$).

The strong blue shift observed upon protonation of the dimethylamino group is a characteristic of the dansyl group and is due to destabilization of the charge transfer state [7].

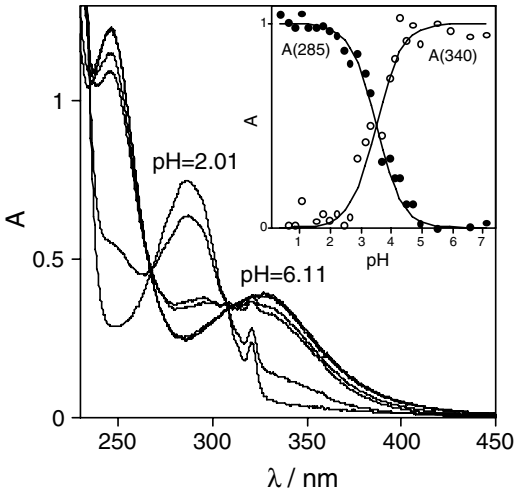

Fig. 1. Absorption spectra of 1.6×10^{-4} M model compound **L3** in 0.15 M NaCl solution; inset: fitting of the absorbance at 285 nm (●) and 340 nm (○).

The emission spectra of compound **L3** upon excitation at the isosbestic point at 308 nm are plotted in Fig. 2 as a function of pH. The spectra are dominated by the presence of an emission band centred at 577 nm. The decrease in emission intensity with decreasing pH (see inset in Fig. 2) fits with a $pK_a = 3.5$, in full agreement with the data from absorption spectrophotometric titration.

The observed emission is characteristic of dansylamide and its derivatives that typically show intense and broad luminescence bands in the 400–600 nm region. These bands are very sensitive to the polarity of the solvent and have considerable charge-transfer character, caused by mixing of the ^1L_a and ^1L_b states of naphthalene with a charge-transfer state arising from the promotion of a lone pair electron on the amino group into a π^* antibonding orbital of the naphthalene ring [7].

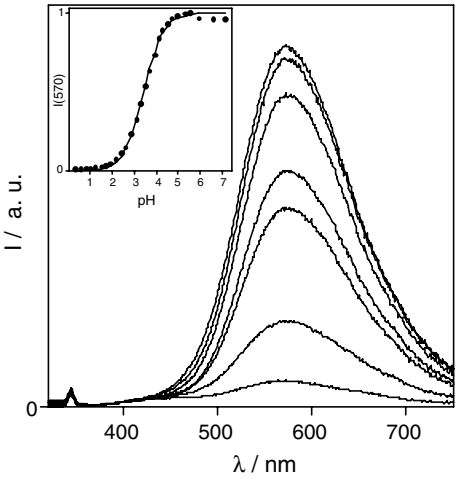

Fig. 2. Fluorescence emission spectra of 1.6×10^{-4} M model compound **L3** in 0.15 M NaCl solution with $\lambda_{exc} = 308$ nm; inset: fitting of the emission intensity at 570 nm.

Table 3
Photophysical properties of the fully unprotonated species of compounds **L1**, **L2** and **L3** in 0.15 M NaCl at pH > 10

	L1	L2	L3
λ_{max} (nm)	328	326	325
ε (M^{-1} cm^{-1})	3180	3880	2400[a]
λ_{em} (nm)	592	532	577
Φ_f	0.12	0.14	0.10
τ (ns)	2.6	3.8	3.1

[a] This value is underestimated due to solubility problems.

Fluorescence decays were obtained with excitation at 339 nm and collection at 520 nm. Above pH 6, the decays were fitted with a single exponential decay law with a decay time $\tau = 3.1$ ns; for pH < 6, an additional shorter component arises with a decay time of ~0.2 ns whose weight increases concomitantly with the decrease of the weight of the longer decay time component.

3.3.2. Dansyl ligand *L1*

The absorption spectra of ligand **L1** as a function of pH are very similar to those of model compound **L3** (see Table 3 and Supplementary material, Fig. 1S). From the spectrophotometric titration, a pK_a value of 3.6 was obtained, in full agreement with the potentiometric data presented above and very close to the pK_a of parent compound **L3**.

The fluorescence emission spectra of ligand **L1** are plotted in Fig. 3a as a function of pH. There are two bands at acidic pH values, one centered at 325 nm and the other at 610 nm, the former decreasing and the latter increasing in intensity with increasing pH, as shown more clearly in Fig. 3b. The data is adequately fitted with the constants obtained by potentiometry.

The band at 325 nm clearly originates from the $\mathbf{L1H_3}^{3+}$ species and strongly resembles the emission spectra of naphthalene derivatives [29,30]. The band at 610 nm originates from the charge transfer state of the deprotonated dansyl unit and its intensity and emission maximum depend on the protonation degree of the ligand. There is a clear red-shift of the emission maxima on going to lower pH values (that is also present in **L2**).

The more emissive species is the fully unprotonated form of **L1**. On the other hand, the less emissive species is the fully protonated form where the dimethylamino group is protonated. An interesting feature is the fact that protonation of the two primary amino groups leads to a decrease in fluorescence in the pH range from 10 to 7. This is apparently surprising since protonation of aliphatic amines in polyamine based fluorescent sensors usually blocks the quenching due to electron transfer from the lone pair of unprotonated amines to aromatic excited states [2,31,32]. In the present studied system, it is likely that intramolecular excited state proton transfer (ESIPT) occurs from the protonated aliphatic primary amino groups to the unprotonated dimethylamino group of the dansyl fluorophore through some stabilized hydrogen-

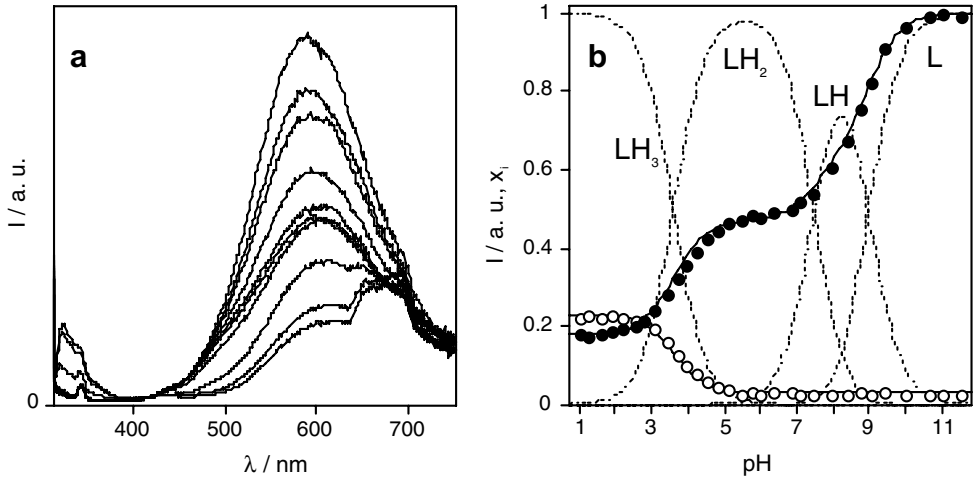

Fig. 3. Fluorescence emission spectra ($\lambda_{exc} = 308$ nm) of 3.08×10^{-5} M **L1** in 0.15 M NaCl solution (a) and respective emission intensity at $\lambda_{em} = 325$ nm (○) and $\lambda_{em} = 585$ nm (●) as a function of pH (b). The emission intensities were normalized to be superposed to the molar fraction distribution of species $(x_i) \cdot N$.

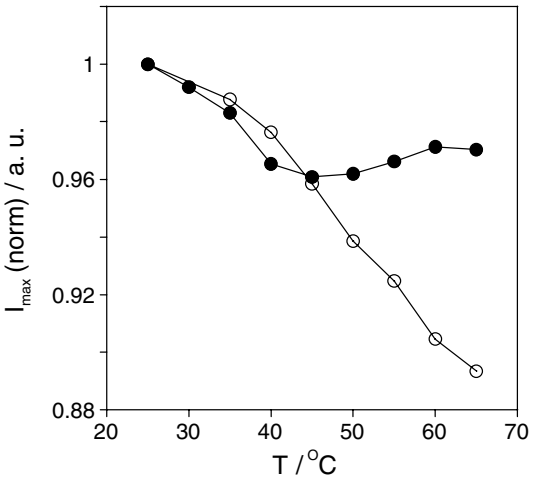

Fig. 4. Temperature dependence of the fluorescence intensity for ligand **L1** ($\lambda_{em} = 592$ nm) (●) and model compound **L3** ($\lambda_{em} = 575$ nm) (○) in 0.15 M NaCl at pH 6.2.

bonded conformer.[1] In this way, on going to more basic pH values, the excited dansyl fluorophore is partially quenched by ESIPT, exhibiting its full fluorescence only for pH > 10 where this mechanism can no longer operate.

If such is the case, an increase in temperature will render the highly oriented H-bond interaction unfavorable, leading to its disruption at sufficiently high temperatures with concomitant disappearance of the quenching arising from ESIPT. Fig. 4, where the fluorescence intensity at the emission maximum of **L1** at a pH in the intermediate plateau of Fig. 3b is presented as a function of temperature, illustrates this effect. For comparison purposes, also the intensity values for the parent compound **L3** are presented. As expected, the fluorescence intensity of the parent compound decreases continuously with increasing temperature, as a result of the increase in the non-radiative pathway for excited state deactivation. On the contrary, compound **L1** containing protonated secondary amines that enable ESIPT to occur, shows an abnormal behaviour with temperature, with a slight increase at temperatures above 45 °C. This is the result of the disruption of the pre-formed H-bond in the ESIPT conformer that leads to a substantial reduction in quenching.

Time resolved fluorescence measurements were collected at selected pH values. At pH 1, the fluorescence decay ($\lambda_{exc} = 280$ nm) collected at $\lambda_{em} = 335$ nm is essentially dominated by a decay time of 0.2 ns, corresponding to the fully protonated form of the ligand. Between pH 4.3 and pH 10.0, the global analysis of the fluorescence decays at different pH values (collected at 520 nm) yields two decay times, $\tau_1 = 1.6$ ns and $\tau_2 = 2.6$ ns, whose relative weights change with pH as depicted in Fig. 5. The species associated with the decay time of 1.6 ns, predominant at pH ~ 4, corresponds to the species where ESIPT is operating while the species with longer decay time is predominant for pH > 10.

3.3.3. Dansyl ligand *L2*

The absorption spectra of ligand **L2** are presented in Fig. 6a. Besides the characteristic absorption features of protonated and unprotonated dansyl group, an additional band at 260 nm is present due to the absorption of the pyridine units. Interpolation of the absorption titration profiles of the whole spectrum allows the determination of the protonation constants of **L2** and the recovery of the absorption spectra of the several acido-basic forms of the

[1] At these pH values, the proton concentration is too low to allow efficient excited state proton transfer from the solvent. Assuming a diffusional rate constant ($\sim 10^{10}$ M s^{-1}) for the encounter and a proton concentration of 10^{-8} M, the pseudo-unimolecular rate constant for intermolecular ESPT is 10^2 s^{-1} that cannot compete with the excited state deactivation of ~1/2 ns = 5×10^9 s^{-1}.

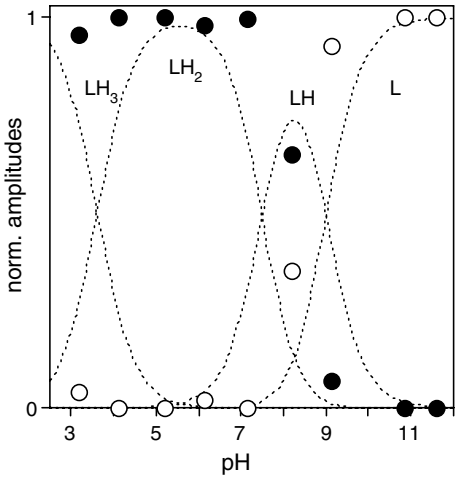

Fig. 5. pH dependence of the amplitudes associated to $\tau_1 = 1.6$ ns (●) and $\tau_2 = 2.6$ ns (○) obtained from global fitting of fluorescence decays of ligand **L1** in 0.15 M NaCl; $\lambda_{exc} = 339$ nm; $\lambda_{em} = 520$ nm.

ligand (Fig. 6b). The two first protonation constants involve the two secondary amines and lead only to very small changes in the absorption spectra. The data was thus analyzed by fixing the values of these constants as obtained from potentiometry ($\log K_1 = 7.98$, $\log K_2 = 6.31$). With this procedure, values of $\log K_3 = 3.65$ and $\log K_4 = 1.5$ were obtained. The first (K_3) corresponds to the protonation of the dansyl group as shown by the absorption spectra of $\mathbf{L2H_3^{3+}}$ and agrees with the value from potentiometric data ($\log K_3 = 3.73$). The second is accompanied by an increase in absorbance at ~260 nm and corresponds to the protonation of one of the pyridines (the second pyridine would require even lower pH values). The order of protonation of ligand **L2** is represented in Scheme 3.

The fluorescence properties of ligand **L2** are very similar to those of **L1** (see Supplementary material, Fig. 2S): the most emissive species is the fully deprotonated form; the mono and diprotonated forms are quenched by ESIPT from the protonated secondary amino groups to the dimethylamino group, until the triprotonated form is reached. Time resolved fluorescence measurements in the intermediate pH region confirm the same behavior as **L1**: the data can be fitted with two decay times (see Supplementary material, Fig. 3S).

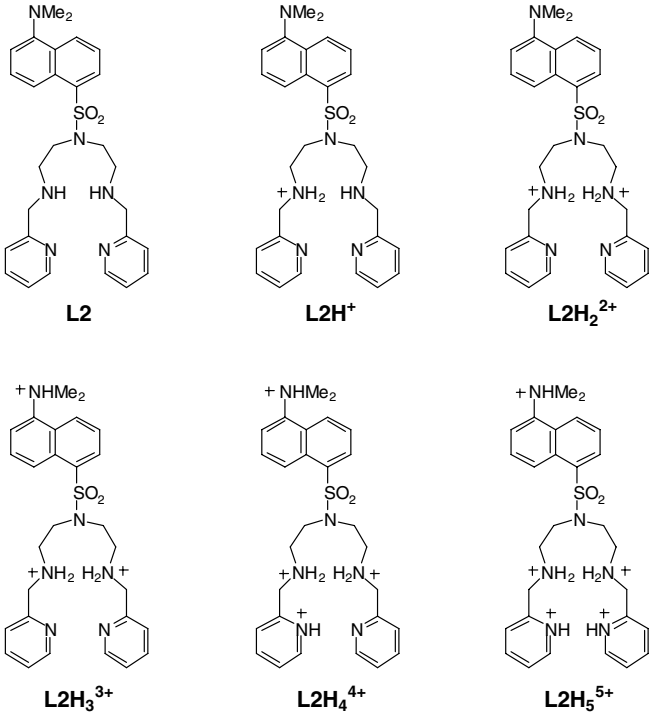

Scheme 3.

Contrary to ligand **L1** that poorly binds Zn(II), ligand **L2** shows appreciable binding constants towards this metal cation, as above described for **L2**.

For the Zn:**L2** (1:1) complex, the absorption spectra are very similar to those of free **L2** (see Supplementary material, Fig. 4S). The comparison between the fluorescence titration curves of the free ligand and the Zn(II) complex shows a decrease of fluorescence emission

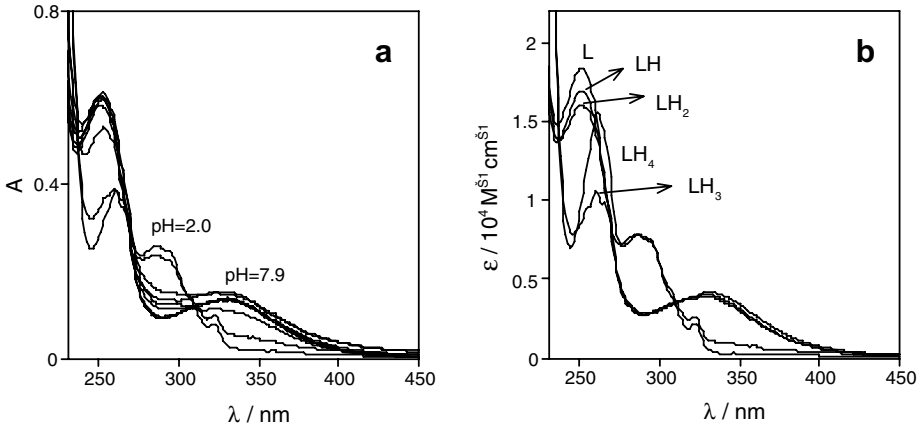

Fig. 6. Absorption spectra of 4.3×10^{-5} M **L2** in 0.15 M NaCl solution as a function of pH (a) and of the different species of the ligand recovered from the fitting of the spectral evolution with pH (b).

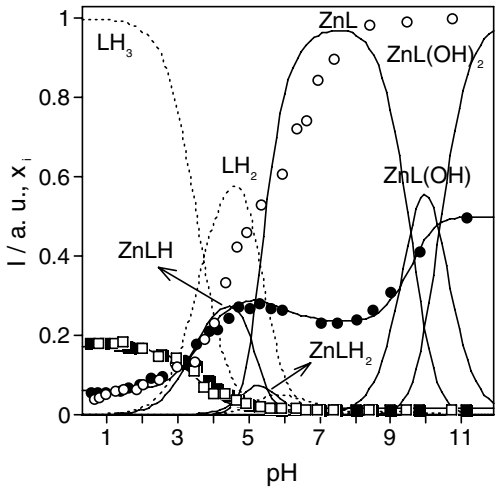

Fig. 7. Steady state fluorescence emission titration curves of 4.3×10^{-5} M **L2** in the presence of Zn(II) (1:1) in 0.15 M NaCl solution, obtained with $\lambda_{exc} = 308$ nm, and followed at $\lambda_{em} = 333$ nm (■) and 575 nm (●). Also shown are the fluorescence emission titration curves for the free ligand (□ and ○). The emission intensities were normalized to be superposed to the molar fraction distribution of species, x_i.

intensity upon coordination with Zn(II), denoting the existence of a CHEQ (chelating enhancement of the quenching) effect in a pH range (6.5–8.5) with great biological interest (Fig. 7). The quenching observed for pH > 4 should be related with the coordination of Zn(II) with the two nitrogens of the pyridine groups and the two nitrogens of the secondary amines. It is known that pyridines, when protonated or complexed to Zn(II), efficiently quench aromatic fluorophores such as naphthalene and anthracene [33–36]. The increase in fluorescence upon formation of the hydroxo complexes should be related to geometry changes that weaken pyridine coordination or even lead to pyridine decoordination in the case of the bis(hydroxocomplex). This suggests the exploitation of the Zn(II) complex of **L2** as an anion sensor, a work that is in progress.

Ligand **L2** was also titrated in the presence of Cu(II) (1:1) with the appearance of strong quenching of the emission, as commonly observed (Supplementary material, Table 1S, Fig. 5S) [32].

Acknowledgements

Spanish MCYT under Project No. BQU-2003-09215-CO3 and Portuguese FCT-MCTES under Project No. POCTI/QUI/47357/2002 are acknowledged for financial support. J. Pina acknowledges FCT-MCTES for Ph.D. Grant SFRH/BD/18876/2004.

Appendix A. Supplementary material

Supplementary data associated with this article can be found, in the online version, at doi:10.1016/j.ica.2006.11.006.

References

[1] J.P. Desvergne, A.W. Czarnik (Eds.), Chemosensors of Ion and Molecule Recognition, Kluwer, Dordrecht, 1997.
[2] A.P. de Silva, H.Q.N. Gunaratne, T. Gunnlaugsson, A.J.M. Huxley, C.P. McCoy, J.T. Rademacher, T.E. Rice, Chem. Rev. 97 (1997) 1515.
[3] L. Fabbrizzi (Guest Ed.) Chem. Rev. 205 (2000).
[4] A. Bianchi, K. Bowman-James, E. García-España (Eds.), The Supramolecular Chemistry of Anions, Wiley, New York, 1997.
[5] Paul D. Beer, Philip A. Gale, Angew. Chem., Int. Ed. Engl. 400 (2001) 486.
[6] V. Amendola, D. Esteban-Gómez, L. Fabrizzi, M. Licchelli, Acc. Chem. Res. 39 (2006) 343.
[7] Y.-H. Li, L.-M. Chan, L. Tyer, R.T. Moody, C.M. Hirnel, D.M. Hercules, J. Am. Chem. Soc. 97 (1975) 3118.
[8] (a) R. Metivier, I. Leray, B. Lebeau, B. Valeur, J. Mater. Chem. 15 (2005) 2965;
(b) R. Metivier, I. Leray, B. Valeur, Chem. Eur. J. 10 (2004) 4480;
(c) R. Metivier, I. Leray, B. Valeur, Photochem. Photobiol. Sci. 3 (2004) 374.
[9] (a) L. Prodi, M. Montalti, N. Zaccheroni, F. Dallavalle, G. Folesani, M. Lanfranchi, R. Corradini, S. Pagliari, R. Marchelli, Helv. Chim. Acta 84 (2001) 690;
(b) L. Prodi, F. Bolletta, M. Montalti, N. Zaccheroni, Eur. J. Inorg. Chem. (1999) 455.
[10] G.K. Walkup, B. Imperiali, J. Am. Chem. Soc. 119 (1997) 3443.
[11] (a) C.-F. Chen, Q.-Y. Chen, Tetrahedron Lett. 45 (2004) 3957;
(b) R. Miao, Q.-Y. Zheng, C.-F. Chen, Z.-T. Huang, Tetrahedron Lett. 45 (2004) 4959.
[12] S.-Y. Liu, Y.-B. He, G.-Y. Qing, K.-X. Xu, H.-J. Qin, Tetrahedron: Asymmetry 16 (2005) 1527.
[13] S. Pagliari, R. Corradini, G. Galaverna, S. Sforza, A. Dossena, M. Montalti, L. Prodi, N. Zaccheroni, R. Marchelli, Chem. Eur. J. 10 (2004) 2749.
[14] (a) P. Ceroni, V. Vicinelli, M. Maestri, V. Balzani, S.K. Lee, J. van Heyst, M. Gorka, F. Vögtle, J. Organomet. Chem. 689 (2004) 4375;
(b) V. Balzani, P. Ceroni, S. Gestermann, M. Gorka, C. Kauffmann, F. Vögtle, Tetrahedron 58 (2002) 629;
(c) V. Balzani, P. Ceroni, S. Gestermann, C. Kauffmann, M. Gorka, F. Vögtle, Chem. Commun. (2000) 853;
(d) F. Vögtle, S. Gestermann, C. Kauffmann, P. Ceroni, V. Vicinelli, L. DeCola, V. Balzani, J. Am. Chem. Soc. 121 (1999) 12161.
[15] P.L. Anelli, L. Lunazzi, F. Montanari, S. Quici, J. Org. Chem. 49 (1984) 4197.
[16] G.H. Seare, S.F. Lincoln, S.G. Teague, D.G. Rowe, Aust. J. Chem. 32 (1979) 519.
[17] Yuen Ng, R.J. Motekaitis, A.E. Martell, Inorg. Chem. 18 (1979) 2982.
[18] E. García-España, M.-J. Ballester, F. Lloret, J.-M. Moratal, J. Faus, A. Bianchi, J. Chem. Soc., Dalton Trans. (1988) 101.
[19] M. Fontanelli, M. Micheloni, in: Proceedings of the I Spanish-Italian Congress on Thermodynamics of Metal Complexes, Diputación de Castellón, Castellón, Spain, 1990.
[20] (a) G. Gran, Analyst 77 (1952) 661;
(b) F.J. Rossotti, H. Rossotti, J. Chem. Educ. 42 (1965) 375.
[21] P. Gans, A. Sabatini, A. Vacca, Talanta 43 (1996) 1739.
[22] Hyperquad Simulation and Speciation (HySS). © 2006 Protonic Software. P. Gans, Protonic Software, 2 Templegate Avenue, Leeds LS15 0HD, England.
[23] J.N. Demas, G.A. Crosby, J. Phys. Chem. 75 (1971) 991.
[24] J. Seixas de Melo, P.F. Fernandes, J. Mol. Struct. 565 (2001) 69.
[25] G. Striker, V. Subramaniam, C.A.M. Seidel, A. Volkmer, J. Phys. Chem. B 103 (1999) 8612.
[26] R. Aucejo, J. Alarcón, E. García-España, J.M. Llinares, K.L. Marchin, C. Soriano, C. Lodeiro, M.A. Bernardo, F. Pina, J. Pina, J. Seixas de Melo, Eur. J. Inorg. Chem. (2005) 4301.

[27] M. Montalti, L. Prodi, N. Zaccheroni, G. Fali, J. Am. Chem. Soc. 124 (2002) 13540.
[28] S. Aoki, H. Kawatani, T. Goto, E. Kimura, M. Shiro, J. Am. Chem. Soc. 123 (2001) 1123.
[29] I.B. Berlman, Handbook of Fluorescence Spectra of Aromatic Molecules, 2nd ed., Academic Press, London, 1971.
[30] J. Malkin, Photophysical and Photochemical Properties of Aromatic Compounds, CRC Press, Boca Raton, 1992.
[31] A.W. Czarnik, Acc. Chem. Res. 27 (1994) 302.
[32] (a) F. Pina, J.C. Lima, C. Lodeiro, J. Seixas de Melo, P. Diaz, M.T. Albelda, E. García-España, J. Phys. Chem. A 106 (2002) 8207; (b) F. Pina, M.A. Bernardo, E. García-España, Eur. J. Inorg. Chem. 10 (2000) 2143.
[33] A.P. de Silva, H.Q.N. Gunaratne, C.P. McCoy, Chem. Commun. 21 (1996) 2399.
[34] L. Fabbrizzi, F. Gatti, P. Pallavicini, L. Parodi, New J. Chem. (1998) 1403.
[35] S.A. de Silva, A. Zavaleta, D.E. Baron, O. Allam, E.V. Isidor, N. Kashimura, J.M. Percarpio, Tetrahedron Lett. 38 (1997) 2237.
[36] R. Aucejo, J. Alarcón, E. García-España, J.M. Llinares, K.L. Marzgin, C. Soriano, M.A. Bernardo, F. Pina, J. Pina, J. Seixas de Melo, Eur. J. Inorg. Chem. (2005) 4301.